Fundamental Research 6 (2026) 718–724

Contents lists available at ScienceDirect

Fundamental Research

journal homepage: http://www.keaipublishing.com/en/journals/fundamental-research/

Article

Wavelength-selective thermal nonreciprocity barely improves sky radiative cooling ☆

Zihe Chen [a,1], Shilv Yu [a,1], Jinlong Ma [a], Bin Xie [b], Sun-Kyung Kim [c,*], Run Hu [a,c,d,*]

[a] School of Energy and Power Engineering, Huazhong University of Science and Technology, Wuhan 430074, China
[b] School of Mechanical Science and Engineering, Huazhong University of Science and Technology, Wuhan 430074, China
[c] Department of Applied Physics, Kyung Hee University, Yongin-si, Gyeonggi-do 17104, Republic of Korea
[d] Wuhan National Laboratory for Optoelectronics, Huazhong University of Science and Technology, Wuhan 430074, China

ARTICLE INFO

Article history:
Received 4 December 2024
Received in revised form 18 December 2024
Accepted 29 December 2024
Available online 6 January 2025

Keywords:
Radiative cooling
Sky radiative cooling
Nonreciprocal thermal radiation
Thermal nonreciprocity
Wavelength selectivity

ABSTRACT

Sky radiative cooling has showcased great potential for passive refrigeration without extra energy consumption, while its cooling power and efficiency are confined by Kirchhoff's law, that is, the emissivity is equal to the absorptivity. The recent development of thermal nonreciprocity that breaks the limitations of Kirchhoff's law, especially in a broadband manner, makes nonreciprocal radiative cooling (NRC) possible. However, as there are few reports on NRC either theoretically or experimentally, it is necessary to evaluate the feasibility and worthiness of developing NRC. Here, we discussed the effects of NRC at around room temperature (298.15 K) from three perspectives: ideal selective radiators, non-selective radiators, and colored radiators, which are the current primary radiative coolers. Counterintuitively, we found that introducing thermal nonreciprocity barely improves sky radiative cooling, and only in the atmospheric window (8–13 μm) even leads to a negative gain. The current findings break the intuition of NRC and offer a negative proof for the development of NRC devices.

1. Introduction

Sky radiative cooling (RC) has garnered increasing attention in both academics and industry as an emerging zero-energy input cooling technology that continuously radiates thermal energy into the low-temperature outer space mainly through the atmospheric window (8–13 μm), thereby reducing the temperature of objects passively [1,2]. RC has broad application prospects in many fields, such as thermal management and building energy conservation [3,4], just to name a few. To achieve sky RC, various materials and structures have been proposed, such as photonic crystals [5], films [6], coating [7], wood [8], ceramics [9], fibers [10], metasurfaces [11], and metamaterials [12], and most of them regulate the reflectivity and emissivity spectra such as to achieve high reflectivity in the solar band and high emissivity in the atmospheric window, which is the basic rule for spectral regulation for sky RC, as shown in Fig. 1a. At present, two types of radiative coolers have been extensively discussed: one with high emissivity across the entire mid-infrared band (Non-Selective), and the other with selective high emissivity only within the atmospheric window (Selective) [12]. With a wider emission bandwidth, the former emits more energy but suffers from more atmosphere absorption than the latter due to the equal absorptivity and emissivity according to Kirchhoff's law [13]. Such an equal relationship between absorptivity and emissivity, $\epsilon(\theta, \lambda) = \alpha(\theta, \lambda)$, as described by Kirchhoff's law, is also called the reciprocal principle of thermal radiation, which results in inevitable thermal absorption from the environment and kind of deteriorates the RC performance.

Fortunately, such severe requirements of Kirchhoff's law can be broken by experimentally applying magneto-optical (MO) material or Weyl semimetal without violating the laws of thermodynamics [14–24], i.e., $\epsilon(\theta, \lambda) \neq \alpha(\theta, \lambda)$. Such thermal nonreciprocity affirmatively provides a new degree of freedom in thermal radiation control and enables more flexible regulation technologies in thermal energy management. For example, the conventional reciprocal single-junction photovoltaic (PV) efficiency limit is the Shockley–Queisser limit (33% for single-junction silicon PV cell) [25,26]. To break this limit, the configuration of multi-junction reciprocal PV cells has been proposed, but the maximum efficiency can only approach the multicolor limit of 86.8% due to the reciprocity. The introduction of thermal nonreciprocal can further break the efficiency limit of PV cells, reaching the Landsberg limit of 93.3% [27]. In addition, thermal nonreciprocity has also shown a positive role in solar thermal photovoltaics [28] and thermal photovoltaics [29].

As both sky RC and thermal nonreciprocity are fundamentally and technologically important [30–32], there is an open question: will ther-

☆ Peer review under the responsibility of Editorial Board of Fundamental Research.

* Corresponding authors.
E-mail addresses: sunkim@khu.ac.kr (S.-K. Kim), hurun@hust.edu.cn (R. Hu).

[1] These authors contributed equally to this work.

https://doi.org/10.1016/j.fmre.2024.12.019

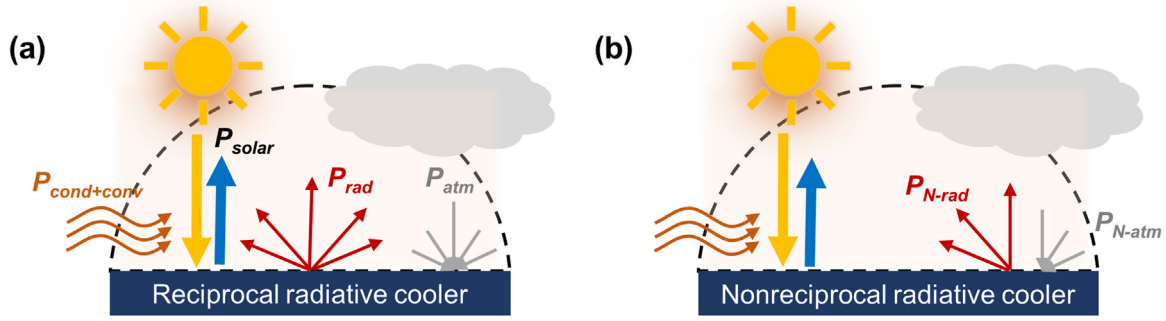

Fig. 1. Schematics of (a) reciprocal and (b) nonreciprocal RC. For reciprocal radiative cooler, external radiation and atmospheric environment absorption are carried out in hemispherical space. For nonreciprocal radiative cooler, in the nonreciprocal band, there is only half of the external radiation and half of the atmospheric absorption when $\epsilon(\theta) = 1$ and $\alpha(\theta) = 0$.

mal nonreciprocity improve RC performance just like in the PV field? Intuitionally, thermal nonreciprocity helps the improvement of sky RC due to the decrease of atmospheric absorption. However, due to the mechanism of thermal nonreciprocity and energy conservation principle [33], $\epsilon(\theta) = 1$ and $\alpha(\theta) = 0$, as shown in Fig. S1, can be achieved only within one-half of the incident angle range, while $\epsilon(-\theta) = 0$ and $\alpha(-\theta) = 1$ will be caused at the other half of the incident angle range. As a result, it is difficult to draw a direct conclusion of whether or not thermal non-reciprocity will benefit RC. As far as we know, few studies are focusing on the comprehensive evaluation of the benefit of combining thermal nonreciprocity and sky RC.

In this work, we introduce the concept of thermal nonreciprocity into the ideal selective radiator (SR), non-selective radiator (NSR), and even colored radiator (CR) respectively, and discuss how thermal nonreciprocity affects the sky RC in different nonreciprocal bands. Detailed NRC modeling and discussion of the sky RC performance with and without thermal nonreciprocity are presented.

2. Theoretical calculation model of radiative cooling

The radiator has an area A and a temperature T_e, facing the sky in the normal direction towards the zenith. In addition, the complex environment of the cooler is simplified, only considering the standard sun and breeze environment. With such a setup, its net cooling power P_{net} can be described as [5,34]

$$P_{net}(T_e) = P_{rad}(T_e) - P_{atm}(T_{amb}) - P_{solar} - P_{cond+conv}(T_e) \tag{1}$$

where P_{rad} is the power emitted from the radiator, P_{atm} is the input power from the atmosphere absorbed by the radiator, P_{solar} is the incident solar power absorbed by the radiator, and the power of the non-radiative heat transfer due to the conductive and convective is described by the $P_{cond+conv}$. T_e and T_{amb} are the temperature of the radiator and the ambient air, respectively. P_{rad} is given by

$$P_{rad}(T_e) = A \int d\Omega \int_0^\infty I_{BB}(T_e, \lambda)\epsilon(\lambda, \theta)\cos\theta d\lambda \tag{2}$$

where ϵ (λ, θ) is the emissivity of the radiator at wavelength λ and angle θ. $\int d\Omega = \int_0^{\pi/2} d\theta \sin\theta \int_0^{2\pi} d\varphi$ is the solid angle integration over a hemisphere and I_{BB} (T_e, λ) is the spectral radiance of a blackbody at temperature T_e and wavelength λ, which is given by the Planck's law:

$$I_{BB}(\lambda, T_e) = \frac{2h_P c^2}{\lambda^5} \frac{1}{\exp(h_P c/\lambda k_B T_e) - 1} \tag{3}$$

where h_P is Planck's constant, k_B is Boltzmann constant and c is the speed of light. The input power from the atmosphere radiation in Eq. 1 is given by

$$P_{atm}(T_{amb}) = A \int d\Omega \int_0^\infty I_{BB}(T_{amb,}\lambda)\alpha(\lambda, \theta)\epsilon_{atm}(\lambda, \theta)\cos\theta d\lambda \tag{4}$$

where α (λ, θ) is the absorption of the radiator at wavelength λ and angle θ. ϵ_{atm} (λ, θ) is the emissivity of the atmosphere, which can be calculated as: $\epsilon_{atm}(\lambda, \theta) = 1 - \tau(\lambda)^{1/\cos\theta}$, here τ (λ) is the transmittance of the atmosphere in the zenith direction. The input solar power is given by

$$P_{solar} = A \cdot G \int_0^\infty \epsilon(\lambda, 0) I_{AM1.5}(\lambda) / \int_0^\infty I_{AM1.5}(\lambda) d\lambda \tag{5}$$

where $I_{AM.15}$ (λ) is the standard AM 1.5 spectrum of solar radiation, and G is the total solar irradiance at 1 KW/m^2. The $P_{cond+conv}$ is given by

$$P_{cond+conv} = A \cdot h(T_{amb} - T_e) \tag{6}$$

where h is a non-radiative heat transfer coefficient that combines the effective conductive and convective heat exchange.

For the nonreciprocal radiator in Fig. 1b, when the incidence angle is 0°, there is no nonreciprocity phenomenon, so the introduction of nonreciprocity does not affect the input solar power and the power of the non-radiative heat transfer, but only affects the power emitted from the radiator and the absorbed power from the atmosphere. Here, considering the nonreciprocal band from λ_1 to λ_2, the power emitted from the radiator under the thermal nonreciprocity $P_{N\text{-}rad}$ is given by

$$P_{N-rad}(T_e) = \frac{1}{2} P_{rad}(T_e) = \frac{A}{2} \int d\Omega \int_{\lambda_1}^{\lambda_2} I_{BB}(T_e, \lambda)\epsilon(\lambda, \theta)\cos\theta d\lambda. \tag{7}$$

The input power from the atmosphere radiation under the thermal nonreciprocity $P_{N\text{-}atm}$ is given by

$$\begin{aligned} P_{N-atm}(T_{amb}) &= \frac{1}{2} P_{atm}(T_{amb}) \\ &= \frac{A}{2} \int d\Omega \int_{\lambda_1}^{\lambda_2} I_{BB}(T_{amb,}\lambda)\alpha(\lambda, \theta)\epsilon_{atm}(\lambda, \theta)\cos\theta d\lambda. \end{aligned} \tag{8}$$

By integrating the above equations separately, we can obtain the net cooling power P_{net} of the radiator at different temperature T_e. When the radiator reaches a thermal equilibrium state, the P_{net} is zero, and the corresponding steady-state temperature T_s can be obtained. A lower T_s indicates a better cooling performance. In the following calculations, without additional explanation, the ambient temperature T_{amb} is set to 298.15 K to simulate a sunny and breezy situation.

3. Theoretical calculation of nonreciprocal radiative cooling

In this section, we will discuss the influence of thermal nonreciprocity on RC from three aspects: 1) The effect of thermal nonreciprocity on the ideal selective radiator (R-8–13); 2) The effect of thermal nonreciprocity on the ideal non-selective radiator (R-2.5–25); 3) Effect of thermal nonreciprocity on color selective/non-selective radiator. Each section considers the influence of different nonreciprocal bands on RC and names the different bands N-4–8, N-8–13, and N-13–25, where the letters N and R represent nonreciprocal and reciprocal, respectively, and the numbers represent the band range.

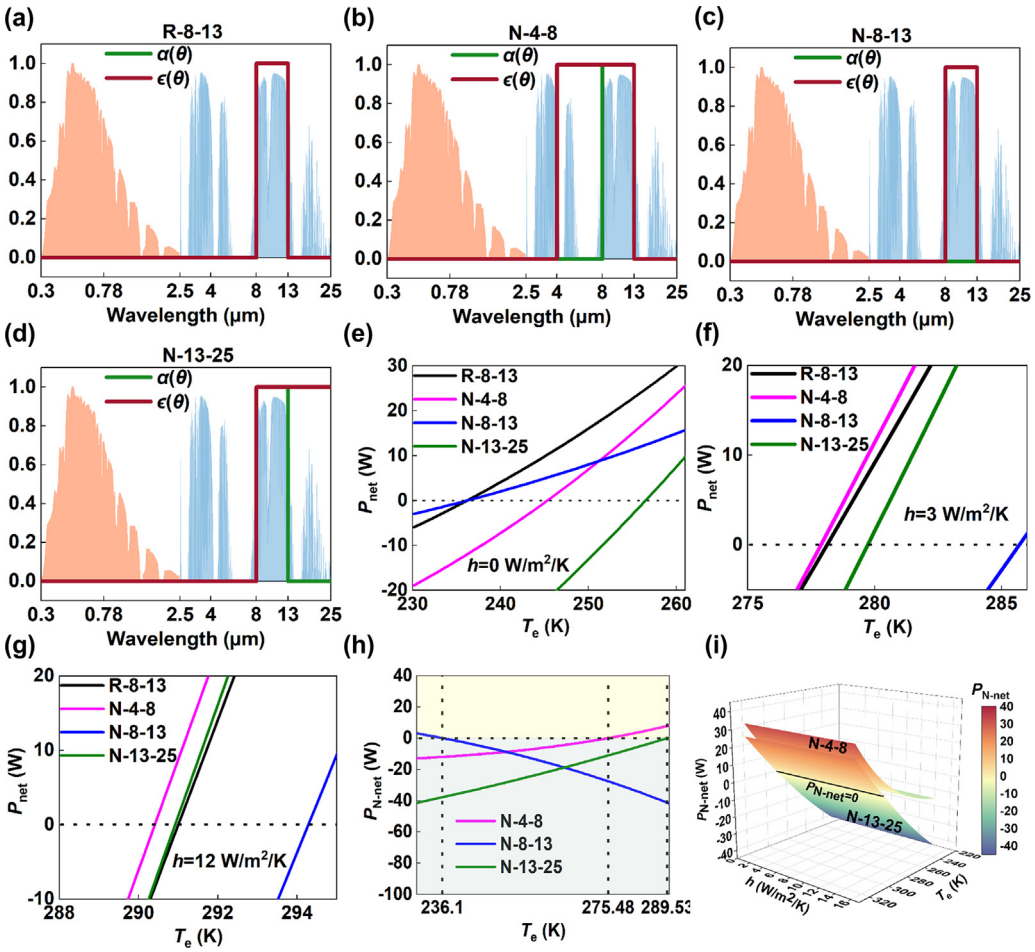

Fig. 2. Ideal spectral absorptivity ($\alpha(\theta)$) and emissivity ($\epsilon(\theta)$) of the selective radiator with $\alpha(\theta) = \epsilon(\theta) = 1$ and the corresponding nonreciprocal radiators with $\alpha(\theta) = 0$ and $\epsilon(\theta) = 1$. (a) R-8–13 with unit emissivity and absorptivity in the band (8–13 μm). (b) N-4–8 with unit emissivity and zero absorptivity in the band (4–8 μm). (c) N-8–13 with unit emissivity and zero absorptivity of in the band (8–13 μm). (d) N-13–25 with unit emissivity and zero absorptivity in the band (13–25 μm). (e) P_{net} of the selective radiator and corresponding nonreciprocal radiators with $h = 0$ W/m^2/K. (f) P_{net} of the selective radiator and corresponding nonreciprocal radiators with $h = 3$ W/m^2/K. (g) P_{net} of the selective radiator and corresponding nonreciprocal radiators with $h = 12$ W/m^2/K. (h) The net power resulting from nonreciprocity with different nonreciprocal bands. (i) Relationship between $P_{N\text{-net}}$ and h of the nonreciprocal radiators (N-4–8 and N-13–25).

3.1. Effect of thermal nonreciprocity on the ideal selective radiator

The theoretical emission and absorption spectra of the ideal selective radiator and their corresponding nonreciprocal radiators with different nonreciprocal bands are shown in Fig. 2a-d. Fig. 2a shows the absorptivity and emissivity spectra of the ideal selective radiator, which has a unit absorptivity/emissivity in the atmospheric window. Fig. 2b-d show the absorptivity and emissivity spectra of the nonreciprocal selective radiators with different nonreciprocal bands. For example, when the nonreciprocal band is 4 to 8 μm, the emissivity is 1 and the absorptivity is 0 in half of the hemisphere, and the absorptivity is 1 and the emissivity is 0 in the other half of the hemisphere space, refer to Fig. 1b and Fig. S1. Fig. 2e-g discuss the effect of different nonreciprocal bands on RC with different h. When $h = 0$ W/m^2/K, R-8–13 has the lowest T_s of about 236.15 K, and the introduction of thermal nonreciprocity in different bands cannot reduce T_s, but increase T_s. When $h = 3$ W/m^2/K, T_s of R-8–13 is 278.12 K and that of N-4–8 is 277.88 K. The latter has a 0.24 K reduction and a higher P_{net} than R-8–13, indicating that the introduction of thermal nonreciprocity in the band of 4–8 μm can slightly help RC. However, the T_s of N-8–13 is equal to 285.7 K, which is higher than that of R-8–13 and shows the weakest cooling performance. As h continues to increase to 12 W/m^2/K, N-4–8 also has the best cooling performance, but even if h increases to 12 W/m^2/K, T_s can only be reduced by about 0.6 K compared with R-8–13, as shown in Fig. 2g. In addition, the T_s of N-13–25 is also slightly lower than that of R-8–13 (about 0.1 K), showing a very limited gain effect. Therefore, for ideal selective radiators, the introduction of thermal nonreciprocity in different bands has limited and even harmful effects on RC.

Here, the influence mechanism of thermal nonreciprocity on RC is analyzed by calculating the net power brought by nonreciprocity. Compared to R-8–13, when the nonreciprocal band is not 8–13 μm, the net power resulting from the nonreciprocity $P_{N\text{-net}}$ is

$$P_{N-net}(T_e) = P_{N-rad}(T_e) - P_{N-atm}(T_{amb}). \quad (9)$$

When the nonreciprocal band is 8–13 μm, the net power resulting from nonreciprocity $P_{N\text{-net}}$ is

$$P_{N-net}(T_e) = P_{N-atm}(T_{amb}) - P_{N-rad}(T_e). \quad (10)$$

According to Eq. 9–10, the relationships between $P_{N\text{-net}}$ and T_e for different nonreciprocal bands are shown in Fig. 2h. For the case of N-4–8, $P_{N\text{-net}}$ is positive when $T_e > 275.48$ K, representing that thermal nonreciprocity can help RC, which explains the higher P_{net} and lower T_s of N-4–8 in Fig. 2f-g. Similarly, when $T_e > 289.53$ K, N-13–25 can also improve cooling performance. However, for the case of N-8–13, $P_{N\text{-net}}$ is negative when $T_e > 236.1$ K, which shows that the introduction of thermal nonreciprocity in 8–13 μm cannot help RC. The relationship between $P_{N\text{-net}}$ and h is further discussed, as shown in Fig. 2i. For exam-

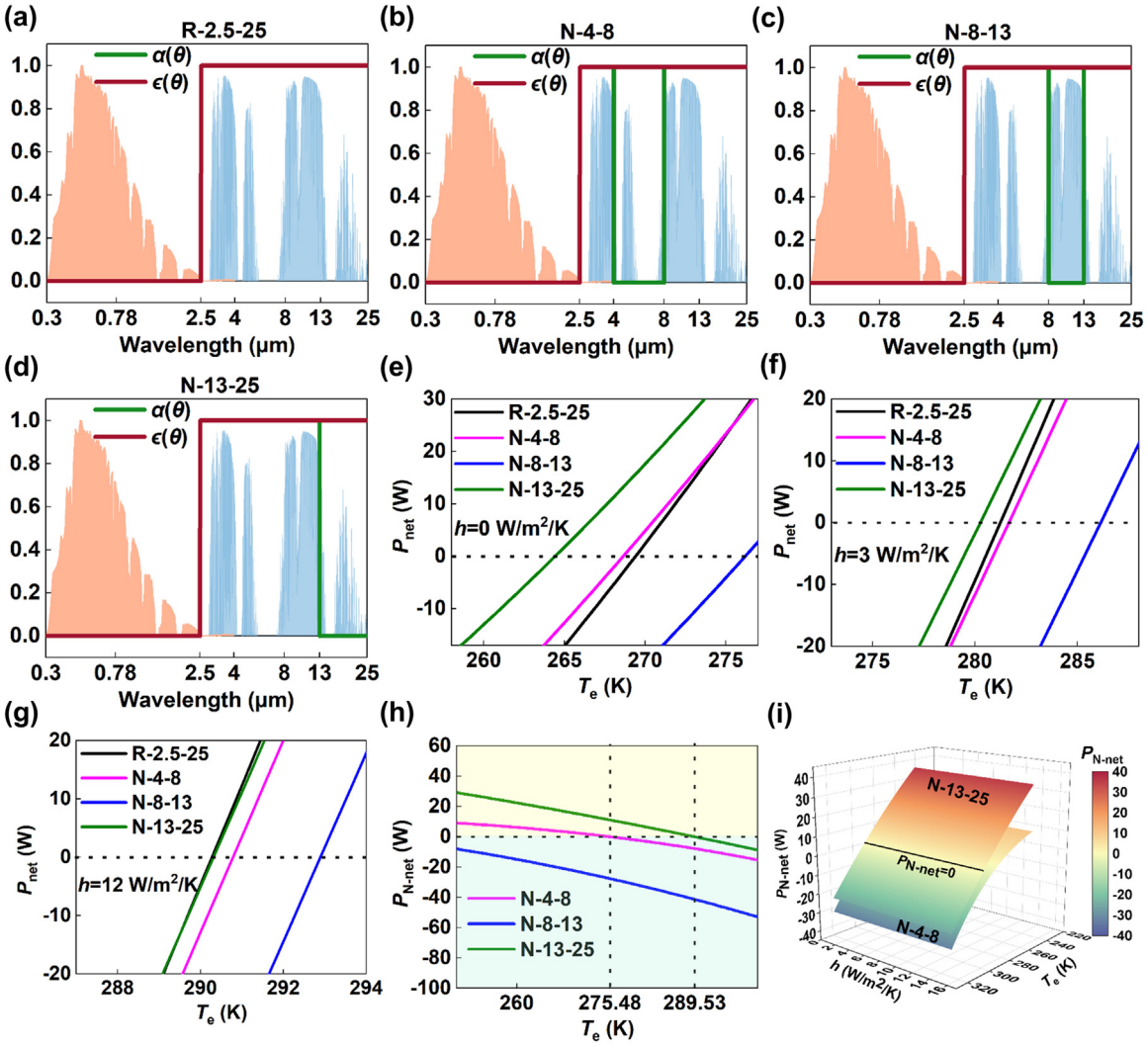

Fig. 3. Ideal spectral absorptivity ($\alpha(\theta)$) and emissivity ($\epsilon(\theta)$) of the non-selective radiator with $\alpha(\theta) = \epsilon(\theta) = 1$ and the corresponding nonreciprocal radiators with $\alpha(\theta) = 0$ and $\epsilon(\theta) = 1$. (a) R-2.5–25 with unit emissivity and absorptivity in the band (8–13 μm). (b) N-4–8 with unit emissivity and zero absorptivity in the band (4–8 μm). (c) N-8–13 with unit emissivity and zero absorptivity in the band (8–13 μm). (d) N-13–25 with unit emissivity and zero absorptivity in the band (13–25 μm). (e) P_{net} of the non-selective radiator and corresponding nonreciprocal radiators with h = 0 W/m^2/K. (f) P_{net} of the non-selective radiator and corresponding nonreciprocal radiators with h = 3 W/m^2/K. (g) P_{net} of the non-selective radiator and corresponding nonreciprocal radiators with h = 12 W/m^2/K. (h) The net power resulting from nonreciprocity with different nonreciprocal bands. (i) Relationship between $P_{N\text{-}net}$ and h of the nonreciprocal radiators (N-4–8 and N-13–25).

Table 1
Effect of different nonreciprocal bands on SR (T_{amb} = 298.15 K).

Cases	Cooling power gain	ΔT_s (h = 12 W/m^2/K)
N-4–8	Positive gain, T_e > 275.48 K	ΔT_s = 0.6 K
N-8–13	Negative gain, T_e > 236.1 K	ΔT_s = −3.3 K
N-13–25	Positive gain, T_e > 289.53 K	ΔT_s = 0.1 K

ple, when $P_{N\text{-}net} = 0$, it is a horizontal line, meaning that $P_{N\text{-}net}$ does not change with h.

To sum up, to show the effect of thermal non-reciprocity more clearly on the selective radiator, it is summarized in Table 1. From the perspective of power gain, when T_e is higher than 275.48 K/289.53 K, the introduction of thermal nonreciprocity in the band of 4–8 μm /13–25 μm can help RC, corresponding to Fig. 2h. From the perspective of equilibrium temperature, for example, when h = 12 W/m^2/K, N-4–8/N-13–25 can achieve the reduction of T_s, but the reduction degree is only 0.6 K/0.1 K, corresponding to Fig. 2g, showing a very limited gain effect. In addition, we note that when T_e > 236.1 K, the introduction of thermal nonreciprocity in the atmospheric window only leads to a reduced RC.

3.2. Effect of thermal nonreciprocity on the ideal non-selective radiator

Next, we investigate the effect of thermal nonreciprocity on non-selective radiators. The theoretical emission and absorption spectra of the ideal non-selective radiator and the corresponding nonreciprocal radiators with different nonreciprocal bands are shown in Fig. 3a-d. Fig. 3a shows the absorptivity and emissivity spectra of the ideal non-selective radiator, which has a unit absorptivity/emissivity in the band of 2.5–25 μm. Fig. 3b-d show the absorptivity and emissivity spectra of the non-reciprocal non-selective radiators with different nonreciprocal bands in half of the hemispherical space. Fig. 3e-g discuss the effect of different nonreciprocal bands on RC with different h. When h = 0 W/m^2/K, N-13–25 has the lowest T_s of about 264.4 K, which is about 5 K lower than that of R-2.5–25 (269.4 K), indicating that the introduction of thermal nonreciprocity in 13–25 μm can help RC for non-selective radiators. In addition, T_s of N-4–8 is about 268.65 K, which is about 0.75 K lower than that of R-2.5–25, which also shows a certain gain effect. However, for the case of N-8–13, T_s is 276.2 K, showing the weakest cooling performance compared with other radiators. When h = 3 W/m^2/K, as shown in Fig. 3f, only N-13–25 still has a better cooling performance than R-

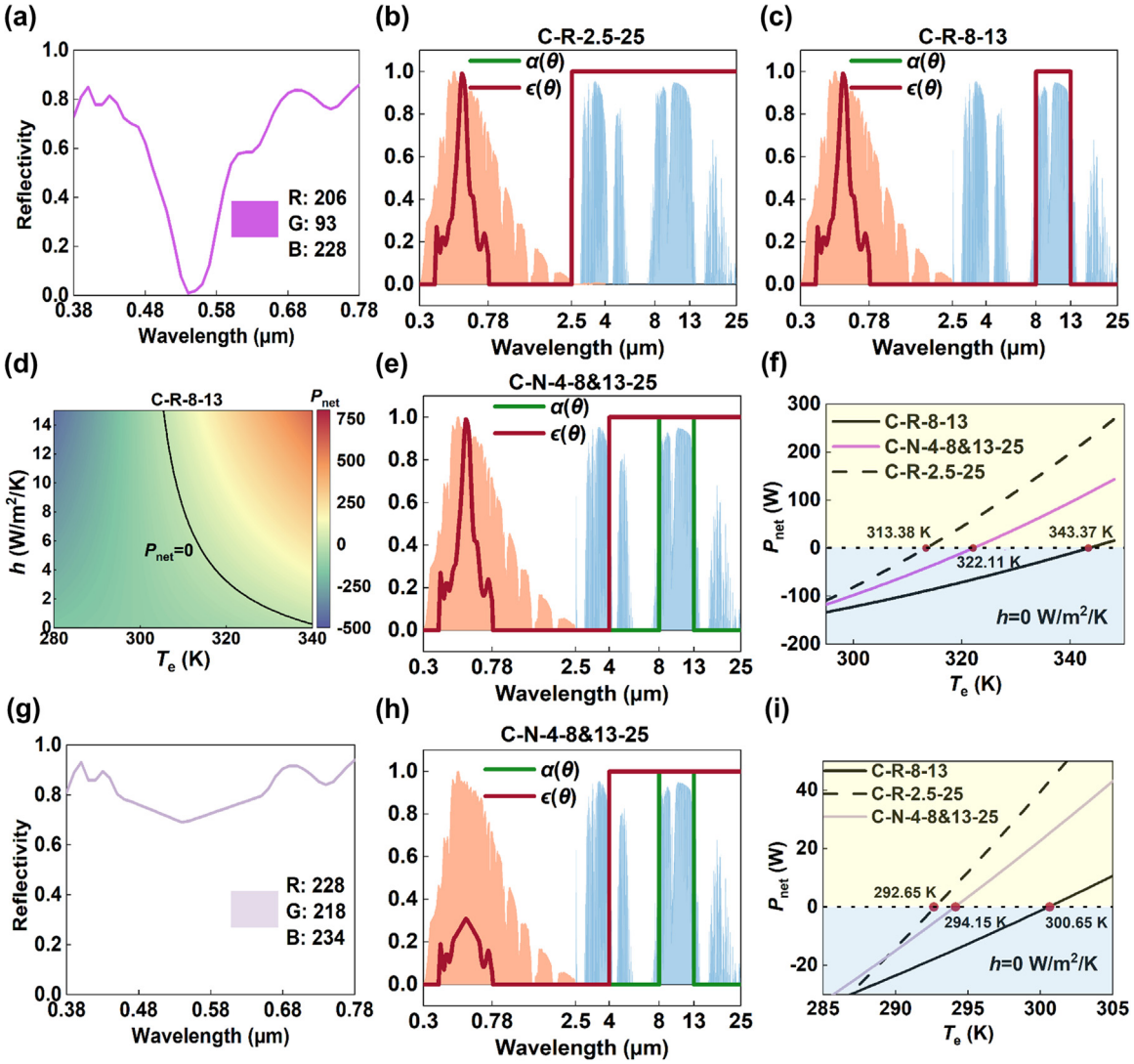

Fig. 4. (a) The reflectance spectral of deep magenta. (b) Reciprocal non-selective radiator with magenta (C-R-2.5–25). (c) Reciprocal selective radiator with magenta (C-R-8–13). (d) Relationship of P_{net} of C-R-8–13 with T_e and h. (e) Nonreciprocal radiator with magenta (C-N-4-8&13-25). (f) Net cooling power of C-R-2.5–25, C-R-8–13 and C-N-4-8&13-25 with h = 0 W/m^2/K. (g) Reflectance spectrum for a light red case. (h) The spectrum of the nonreciprocal color radiator with light red color (C-N-4-8&13-25). (i) Net cooling power of C-R-8–13, C-R-2.5–25 and C-N-4-8&13-25 with h = 0 W/m^2/K for the light red case.

2.5–25, which is about 1 K lower than that of R-2.5–25. As h increases to 12 W/m^2/K, the thermal nonreciprocity hardly helps RC for the non-selective radiator, as shown in Fig. 3g.

Here, the influence mechanism of thermal nonreciprocity on R-2.5–25 is analyzed by calculating the net power brought about by thermal nonreciprocity. Compared to R-2.5–25, the net power resulting from nonreciprocity $P_{N\text{-}net}$ is

$$P_{N-net}(T_e) = P_{N-atm}(T_{amb}) - P_{N-rad}(T_e). \quad (11)$$

According to Eq. 11, the changes of net power with T_e in different nonreciprocal bands are shown in Fig. 3h. For the case of N-4–8, $P_{N\text{-}net}$ is positive when T_e < 275.48 K, representing that thermal nonreciprocity can help RC, which also explains the lower T_s of N-4–8 than that of R-2.5–25 in Fig. 3e. Similarly, for the case of N-13–25, when T_e < 289.53 K, $P_{N\text{-}net}$ is positive, which explains the lower T_s of N-13–25 than that of R-2.5–25 in Fig. 3e-f. However, for the case of N-8–13, $P_{N\text{-}net}$ is negative, which explains why the atmospheric window cannot be selected as the nonreciprocal band. The relationship between $P_{N\text{-}net}$ and h is also further discussed for nonreciprocal radiators, as shown in Fig. 3i. For example, when $P_{N\text{-}net}$ = 0, it is a horizontal line, which means that $P_{N\text{-}net}$ does not change with h.

Table 2
Effect of the nonreciprocal band on the ideal non-selective radiator (T_{amb} = 298.15 K).

Cases	Power gain	ΔT_s (h = 0 W/m^2/K)	ΔT_s (h = 3 W/m^2/K)
N-4–8	Positive gain, T_e < 275.48 K	ΔT_s = 0.75 K	ΔT_s = −0.41 K
N-8–13	Negative gain	ΔT_s = −6.75 K	ΔT_s = −4.91 K
N-13–25	Positive gain, T_e < 289.53 K	ΔT_s = 5 K	ΔT_s = 1 K

To sum up, in order to more clearly show the effect of thermal nonreciprocity on the non-selective radiator, it is summarized in Table 2. From the point of view of power gain, when T_e is lower than 275.48 K/289.53 K, the introduction of thermal nonreciprocity in the band 4–8 μm /13–25 μm can realize a positive gain, corresponding to Fig. 3h. From the perspective of T_s, N-4–8/N-13–25 can achieve the reduction of T_s and the reduction degree is 0.75 K/5 K when h = 0 W/m^2/K, corresponding to Fig. 3e. However, as h gradually increases, the gain effect is gradually weakened and even negative gain. In addition, similar to Section 3.1, the introduction of thermal nonreciprocity in the atmospheric window only compromises the RC.

3.3. Effect of thermal nonreciprocity on colored radiators

Both reciprocal and nonreciprocal radiators discussed above face a new problem, that is, for the purpose of maximizing the RC, they present total reflection in the solar band, which makes the radiators white appearance. The large area of white appearance is terrible for aesthetic requirements and results in the potential for light pollution. Consequently, in pursuit of practicality, colored radiators (CRs) have been developed, which demonstrate rich color but discounted cooling performance [35]. From the perspective of the spectrum, CR shows color because it exhibits partial reflection rather than total reflection in the visible band, which results in the absorption of solar radiation and thus weakens the cooling effect. Since color and cooling performance are a kind of competition, existing reciprocal-based CRs are limited in color richness and most of them display light colors [36,37].

Therefore, in this section, we discuss whether the thermal nonreciprocity will bring benefits to CRs and have a profound impact. Since darker colors tend to have higher absorption of solar energy than light colors, it is difficult to achieve sub-ambient cooling in conventional reciprocal RC [38]. For this purpose, we randomly chose a deep color, namely deep magenta, to explore the effect of thermal nonreciprocity on CRs and determine whether it can achieve a better RC. Of course, other dark colors can also be chosen, such as gray, as shown in Fig. S3, whose conclusions are consistent with those of the dark magenta case. Fig. 4a displays the reflectance spectrum of magenta, which has low reflectance especially in the range of 0.48~0.65 μm and results in high absorptivity (emissivity). Here, we consider the effect of nonreciprocity on the color non-selective radiator (C-R-2.5–25) and color selective radiator (C-R-8–13). Firstly, for C-R-2.5–25, its absorption and emission spectra are shown in Fig. 4b. Both the emissivity and absorption are 1 in the band range of 2.5–25 μm, and the visible light band corresponds to the deep magenta spectrum. Fig. S2 shows the relationship of P_{net} of C-R-2.5–25 (deep magenta) with T_e and h. When P_{net} >0, T_e is higher than 300 K, so both N-4–8 and N-13–25 cannot improve the RC for C-R-2.5–25, according to Table 2. Secondly, for the case of C-R-8–13, its absorption and emission spectra are shown in Fig. 4c. The emissivity and absorption are both 1 in the atmospheric window, and the visible light band corresponds to the deep magenta spectrum. Fig. 4d shows the relationship between P_{net} and h of C-R-8–13 with a deep magenta color. It can be seen that when P_{net} >0, T_e is higher than 300 K. According to Fig. 2h and Table 1, since T_e of C-R-8–13 is higher than 289.53 K, both N-4–8 and N-13–25 can improve the RC and the corresponding nonreciprocal spectra are shown in Fig. 4e. When h = 0 W/m^2/K, the net power of C-R-8–13 and the corresponding nonreciprocal radiator (C-N-4-8&13-25) changes with T_e, as shown in Fig. 4f. The introduction of thermal nonreciprocity can reduce T_s by 21.26 K compared with C-R-8–13, showing better cooling performance. However, the cooling performance of C-N-4-8&13-25 is weaker than that of C-R-2.5–25. Therefore, the design of reciprocal non-selective radiators is better for CRs with a dark color. In addition, it should be noted that as the color of the radiator gradually becomes lighter or even white, the advantage of the non-selective radiator will diminish, as shown in Fig. 4g-i and Fig. S4. This is mainly because when the color is lighter, less solar radiation is absorbed and T_s (P_{net}=0) is lower. As shown in Table 2, when T_s gradually decreases to 289.53 K, the introduction of thermal nonreciprocity into the non-atmospheric window will gradually play a positive gain effect. In addition, with the color radiator light to white, as shown in Fig. S4, the performance of nonreciprocal radiator (N-4–8&13–25) is better than that of non-selective thermal radiator (R-2.5–25) but weaker than that of the selective radiator (R-8–13), which is consistent with Sections 3.1 and 3.2.

4. Conclusion

In this work, we discuss the effects of thermal nonreciprocity on ideal selective radiators, non-selective radiators, and colored radiators. For the three radiators, the introduction of thermal nonreciprocity in the atmospheric window (8–13μm) will be harmful to the RC. In addition, for the selective radiator, when T_e is higher than 275.48 K/289.53 K, the introduction of thermal nonreciprocity in the band of 4–8 μm/13–25 μm can help the RC. However, even if with h = 12 W/m^2/K, the T_s of N-4–8/ N-13–25 is only 0.6 K/0.1 K lower than that of R-8–13, which shows a slight enhancement. For non-selective radiators, when h = 0 W/m^2/K, the introduction of thermal nonreciprocity in the 13–25 μm band can realize an obvious gain effect. However, with the increase of h, the gain effect due to thermal nonreciprocity becomes weaker and even negative. For example, when h = 3 W/m^2/K, the introduction of nonreciprocity only reduces T_s by about 1 K. For color radiators with dark colors, C-R-2.5–25 can realize a better RC compared with nonreciprocal radiators. Considering the weak gain effect and high application requirements like strong magenetic field, we conclude that achieving wavelength-selective NRC may be unnecessary.

Declaration of competing interest

The authors declare that they have no conflicts of interest in this work.

Data availability

Data will be made available on request.

Acknowledgements

The authors would like to acknowledge the financial support by National Natural Science Foundation of China (52422603, 92463311, 52211540005), the Open Project Program of Wuhan National Laboratory for Optoelectronics (2021WNLOKF004), Interdisciplinary Research Program of HUST (5003120094), and Natural Science Foundation of Hubei Province (2023AFA072), and the Fundamental Research Funds for the Central Universities (YCJJ20242102).

Supplementary materials

Supplementary material associated with this article can be found, in the online version, at doi:10.1016/j.fmre.2024.12.019.

References

[1] S. Fan, W. Li, Photonics and thermodynamics concepts in radiative cooling, Nat. Photonics 16 (3) (2022) 182–190.
[2] A.P. Raman, M.A. Anoma, L. Zhu, et al., Passive radiative cooling below ambient air temperature under direct sunlight, Nature 515 (7528) (2014) 540–544.
[3] L. Zhou, H. Song, J. Liang, et al., A polydimethylsiloxane-coated metal structure for all-day radiative cooling, Nat. Sustainability 2 (8) (2019) 718–724.
[4] Y. Peng, L. Fan, W. Jin, et al., Coloured low-emissivity films for building envelopes for year-round energy savings, Nat. Sustainability 5 (4) (2021) 339–347.
[5] M. Lee, G. Kim, Y. Jung, et al., Photonic structures in radiative cooling, Light Sci Appl 12 (1) (2023) 134.
[6] H. Yin, X. Zhou, Z. Zhou, et al., Switchable Kirigami structures as window envelopes for energy-efficient buildings, Research 2023 (4) (2023) 0103.
[7] C. Feng, Y. Lei, X.Q. Huang, et al., Experimental and theoretical analysis of sub-ambient cooling with longwave radiative coating, Renew Energy 193 (2022) 634–644.
[8] T. Li, Y. Zhai, S.M. He, et al., A radiative cooling structural material, Science 364 (6442) (2019) 760.
[9] K.X. Lin, S.R. Chen, Y.J. Zeng, et al., Hierarchically structured passive radiative cooling ceramic with high solar reflectivity, Science 382 (6671) (2023) 691–697.
[10] X. Wang, X. Liu, Z. Li, et al., Scalable flexible hybrid membranes with photonic structures for daytime radiative cooling, Adv. Funct. Mater. 30 (5) (2019) 1907562.
[11] M.M. Hossain, B.H. Jia, M. Gu, A metamaterial emitter for highly efficient radiative cooling, Adv. Opt. Mater. 3 (8) (2015) 1047–1051.
[12] Z.F. Huang, X.L. Ruan, Nanoparticle embedded double-layer coating for daytime radiative cooling, Int. J. Heat Mass Transfer 104 (2017) 890–896.
[13] M.M. Hossain, M. Gu, Radiative cooling: Principles, progress, and potentials, Adv. Sci. 3 (7) (2016) 1500360.
[14] C. Guo, B. Zhao, S. Fan, Adjoint Kirchhoff's law and general symmetry implications for all thermal emitters, Phys. Rev. X 12 (2) (2022) 021023.
[15] A. Ghanekar, J.H. Wang, S.H. Fan, et al., Violation of kirchhoff's law of thermal radiation with space-time modulated grating, ACS Photonics 9 (4) (2022) 1157–1164.

[16] Z. Zhang, X. Wu, C. Fu, Validity of Kirchhoff's law for semitransparent films made of anisotropic materials, J Quant Spectrosc Radiat Transf 245 (2020) 106904.
[17] Z. Chen, S. Yu, B. Hu, et al., Multi-band and wide-angle nonreciprocal thermal radiation, Int. J. Heat Mass Transfer 209 (2023) 124149.
[18] Z. Chen, S. Yu, C. Yuan, et al., Ultra-efficient machine learning design of nonreciprocal thermal absorber for arbitrary directional and spectral radiation, J. Appl. Phys. 134 (20) (2023) 203101.
[19] Z. Chen, S. Yu, C. Yuan, et al., Near-normal nonreciprocal thermal radiation with a 0.3T magnetic field based on double-layer grating structure, Int. J. Heat Mass Transfer 222 (2024) 125202.
[20] K. Shi, Y. Xing, Y. Sun, et al., Thermal vertical emitter of ultra-high directionality achieved through nonreciprocal magneto-optical lattice resonances, Adv. Opt. Mater. 10 (24) (2022) 2201732.
[21] K.J. Shayegan, S. Biswas, B. Zhao, et al., Direct observation of the violation of Kirchhoff's law of thermal radiation, Nat. Photonics 17 (2023) 891–896.
[22] M. Liu, S. Xia, W. Wan, et al., Broadband mid-infrared non-reciprocal absorption using magnetized gradient epsilon-near-zero thin films, Nat. Mater. 22 (2023) 1196–1202.
[23] K.J. Shayegan, B. Zhao, Y. Kim, et al., Nonreciprocal infrared absorption via resonant magneto-optical coupling to InAs, Sci. Adv. 8 (2022) eabm4308.
[24] K. Shi, Y. Sun, R. Hu, et al., Ultra-broadband and wide-angle nonreciprocal thermal emitter based on Weyl semimetal metamaterials, Nanophotonics 13 (5) (2024) 737–747.
[25] M.A. Green, Time-asymmetric photovoltaics, Nano Lett 12 (11) (2012) 5985–5988.
[26] T. Lu, M.J. Li, W.C. Lu, et al., Recent progress in the data-driven discovery of novel photovoltaic materials, J Mater Informatics 2 (2) (2022) 1–44.
[27] Y. Park, B. Zhao, S. Fan, Reaching the ultimate efficiency of solar energy harvesting with a nonreciprocal multijunction solar cell, Nano Lett 22 (1) (2022) 448–452.
[28] S.Jafari Ghalekohneh, B. Zhao, Nonreciprocal Solar Thermophotovoltaics, Phys. Rev. Appl. 18 (3) (2022) 034083.
[29] Y. Park, Z. Omair, S. Fan, Nonreciprocal Thermophotovoltaic Systems, ACS Photonics 9 (12) (2022) 3943–3949.
[30] M.Q. Liu, C.Y. Zhao, Near-infrared nonreciprocal thermal emitters induced by asymmetric embedded eigenstates, Int. J. Heat Mass Tran. 186 (2022) 122435.
[31] J. Wu, Y.M. Qing, Tunable near-perfect nonreciprocal radiation with a Weyl semimetal and graphene, PCCP 25 (13) (2023) 9586–9591.
[32] J. Wu, B. Wu, Z. Wang, et al., Strong nonreciprocal thermal radiation in Weyl semimetal-dielectric multilayer structure, Int. J. Therm. Sci. 181 (2022) 107788.
[33] L. Zhu, S. Fan, Near-complete violation of detailed balance in thermal radiation, Physical Review B 90 (22) (2014) 220301.
[34] W. Xi, Y. Liu, W. Zhao, et al., Colored radiative cooling: How to balance color display and radiative cooling performance, Int. J. Therm. Sci. 170 (2021) 107172.
[35] B. Xie, Y.D. Liu, W. Xi, et al., Colored radiative cooling: Progress and prospects, Mater. Today Energy 34 (2023) 101302.
[36] J.W. Cho, E.J. Lee, S.K. Kim, Full-color solar-heat-resistant films based on nanometer optical coatings, Nano Lett 22 (1) (2022) 380–388.
[37] W. Xi, Y.D. Liu, W.X. Zhao, et al., Colored radiative cooling: How to balance color display and radiative cooling performance, Int. J. Therm. Sci. 170 (2021) 107172.
[38] W. Li, Y. Shi, Z. Chen, et al., Photonic thermal management of coloured objects, Nat. Commun. 9 (2018) 4240.

Author profile

Zihe Chen received his M.E. degree in 2022 from China University of Mining and Technology and majored in power engineering. Currently, he is a doctoral student at Huazhong University of Science and Technology under the supervision of Professor Run Hu. His research interests focus on thermal nonreciprocity, radiative cooling and spectrum regulation.

Shilv Yu received his B.S. degree in 2022 from Huazhong University of Science and Technology and majored in energy and power engineering. Currently, he is a master student at Huazhong University of Science and Technology under the supervision of Professor Run Hu. His research interests focus on machine learning, micro-nano structure design, and thermal radiation spectrum regulation.

Sun-Kyung Kim serves as the director of the Nanophotonics Laboratory in the Department of Applied Physics at Kyung Hee University. He has developed design and research methods for various photonic devices in the ultraviolet, visible, near-infrared, and mid-infrared ranges, electromagnetic manipulation techniques for micro/nano metamaterial devices, as well as experimental processing methods.

Run Hu (BRID: 05579.00.70695) received his bachelor and Ph.D. degrees from Huazhong University of Science and Technology in 2010 and 2015, respectively. He has been a visiting scholar at Purdue University in the United States and a JSPS postdoctoral fellow at the University of Tokyo in Japan. Currently, he is a professor in School of Energy and Power Engineering, Huazhong University of Science and Technology. His main research interests include heat and mass transfer, thermal metamaterials and functional devices, and thermal management of optoelectronic devices.